J|A|C|S
COMMUNICATIONS

Published on Web 01/31/2004

Hybrid Approach to the Synthesis of Highly Luminescent CdTe/ZnS and CdHgTe/ZnS Nanocrystals

James M. Tsay,[†] Malte Pflughoefft,[†,‡] Laurent A. Bentolila,[†] and Shimon Weiss*,[†]

Department of Chemistry and Biochemistry, University of California at Los Angeles, Los Angeles, California 90095

Received October 24, 2003; E-mail: sweiss@chem.ucla.edu

Fluorescent semiconductor nanocrystals (NCs) have size-tunable emissions due to quantum size effects[1] and exhibit a high resistance toward photobleaching. NCs emitting in the far-red and near-infrared regions have garnered much interest for in vivo biological imaging,[2,3] the optoelectronics industry,[4] and therapeutics. Biological imaging should especially be enhanced with infrared probes due to separation from autofluorescence background and increased penetration of excitation and emission light through tissue. Previously reported synthetic routes of low band gap CdTe, CdHgTe, and HgTe NCs in water have shown much promise because of their possibility for a large range of wavelength emissions in the near-IR, tunable not only with size but also with composition (by lowering the band gap with increased mercury content).[4] Nanocrystals synthesized by this method, however, are cytotoxic, unstable, and easily photobleachable in biological environments. In contrast, NC synthesis in trioctylphosphine/trioctylphosphine oxide (TOP/TOPO) at higher temperatures yields cores and shells of better crystallinity. Shells synthesized in these solvents improve both the photostability and quantum yields of the cores dramatically.[6−8] Thus far, there has been much more development of higher band gap shells as well as bioconjugation techniques on TOP/TOPO synthesized NCs than on water-based NCs.[2,9−15] Unfortunately, there is an increased difficulty of incorporating mercury into NCs in organic solvents at high temperature. This is due to the fact that mercury precursors suitable for organic solvents are either highly toxic (dimethylmercury) or are difficult to control, especially at higher temperatures (>100 °C).[5]

Recently, CdTe and HgTe NCs synthesized in water were successfully transferred into organic solvents by exchanging water-soluble ligands to dodecanethiol, a hydrophobic ligand ("phase transfer").[16] We utilized phase transfer to combine the two synthesis methods. This hybrid approach affords a facile growth of shells (grown in organic solvents at high temperature) around cores (synthesized in water), to yield small-diameter, highly luminescent near-IR NCs. Previously established recepies[4,17] were used for the two synthesis steps, with only slight modifications, as described below (and in more detail in Supporting Information). CdTe and CdHgTe cores were synthesized in water by injecting NaHTe solution into a solution containing $Cd(ClO_4)_2 \cdot 6(H_2O)$ and mercaptoacetic acid or 2-aminoethanethiol. Small-diameter cores (∼2.5−3 nm) were grown with emissions ranging from 550 to 690 nm. The emission wavelength could be controlled by varying the amount of mercury precursors injected into the solution. Cores were phase-transferred to dodecanethiol/toluene using a modification of a previously established procedure[16] (Supporting Information). The dodecanethiol-capped cores were precipitated, washed, redissolved in chloroform, and injected into a tributylphosphine and trioctylphosphine oxide mixture. For shell synthesis, a solution consisting of diethyl zinc, hexamethyldisilithiane, and tributylphosphine was injected dropwise into the flask until the completion of the shell at the desired shell thickness. Optionally, dimethyl cadmium was added to the shell solution to ease the large lattice mismatch between the core and shell (∼20%). No noticeable differences in fluorescence emission peak shifts or quantum yields were observed for CdS/ZnS shells.

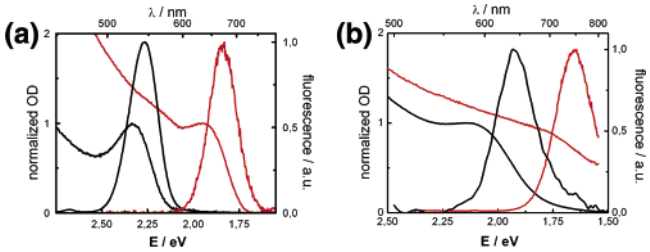

Figure 1. UV/vis absorption and corresponding photoluminescence spectra (a) 2.5 nm CdTe cores before (black) and after (red) shell growth of ZnS; (b) 2.5 nm CdHgTe cores before (black) and after (red) shell growth of ZnS.

A decrease in photoluminescence for both CdTe and CdHgTe cores was observed upon phase transfer. The photoluminescence of the cores was further decreased after injection into a flask of TOPO and tributylphosphine solvents. During the shell synthesis, the quantum yields of the core/shell NCs increased to values similar to those for original cores and higher. Absorption and emission spectra before phase transfer and after shell growth are shown in Figure 1. Accompanied by a large increase in quantum yield (from 20% in water to over 50% in TOPO) of CdTe (initial size of 2.5 nm) is a large red shift of greater than 130 nm (from 550 to 680 nm) in the absorption and emission peaks. Compared to CdTe cores, 2.5 nm ternary cores of CdHgTe with 40:1 Cd:Hg molar content, were red-shifted by 90 nm (from 550 to 640 nm). They were further red-shifted by 110 to 750 nm upon shell growth. A large range of wavelength emissions could be reached from the visible to the near-infrared (from 630 to greater than 800 nm, Supporting Information, Figures S1 and S2) varying the amounts of mercury precursors (core composition) and/or varying the thickness of the shells. It is important to note that the full width half-maximum (fwhm) of the red-shifted photoluminescence peak (red in Figure 1, a and b) did not change appreciably in comparison to the cores (black in Figure 1, a and b). This indicates that there was no significant change in NCs size distribution.

TEM images of both CdTe/ZnS and CdHgTe/ZnS core/shell NCs (Figure 2) indicate that these NCs were monodisperse and maintained small size after shell growth (∼4−5 nm). CdHgTe cores were still crystalline after coating with ZnS (Supporting Information, Figure S3). Evidence for shell growth was provided by elemental analysis using inductively coupled plasma/atomic absorption (ICP/AA). The molar ratio of Zn:S content was found to be close to ∼1. Also, the Cd:Zn ratio was ∼1:2, suggesting a relatively thick

[†] University of California at Los Angeles.
[‡] Current address: Institut für Physikalische Chemie, Universität Hamburg, Germany.

10.1021/ja039227v CCC: $27.50

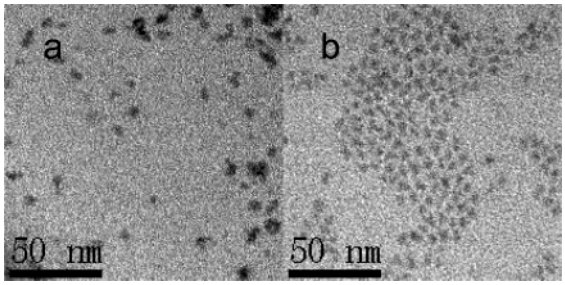

Figure 2. TEM pictures: (a) CdHgTe/ZnS core/shell NCs (emission 750 nm); (b) CdTe/ZnS c ore/shell NCs (emission 680 nm)

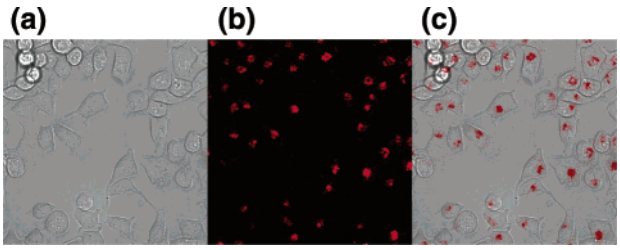

Figure 3. Cell staining of IR-emitting CdHgTe/ZnS NCs in micelles on live P815 mast cells, DIC image of cells (a), confocal microscopy image (b), merge (c). Detection range 650−750 nm.

shell grown over a small CdHgTe core. Finally, the cadmium: mercury content of 40:1 indicates that a small amount of mercury incorporation is enough to considerably red shift the emission.

There are a couple of possibilities for the observed large, permanent red-shifted emission after shell growth. In principle, Ostwald ripening may occur because of nanocrystal surfaces that may have more defects and reactivity due to ligand exchange. This would allow for easier dissolution of some particles and growth of others. If ripening does indeed occur, larger particles will emit longer wavelengths due to reduction in quantum confinement. Initially we used temperatures ranging between 145−170 °C during the shell synthesis (much higher than the reflux temperature of the water-based core synthesis). Dissolution of dodecanethiol-capped cores was observed at the higher CdSe cores, but at much higher temperature. Subsequent reactions were therefore carried out at 145 °C. However, the diameters of the 680 nm emitting core/shell CdTe/ZnS NCs, as measured by TEM (Figure 2), range ∼4−5 nm, i.e. the particles have not grown enough to explain the shift.[17] Furthermore, the fwhm of the photoluminescence peaks does not increase after shell growth (Figure 1), indicating that Ostwald ripening is most likely not the correct explanation for the large shift.

Another possible explanation is lattice strain induced by the shell growth. Indeed, with more shell material added, the larger the red shift is (Supporting Information, Figure S2). The amount of red shift is too large to be explained by the penetration of the electron wave function into the ZnS shell.[7] In previous work, CdSeTe NC cores were shown to have emissions with longer wavelengths than possible in CdTe NCs. This was also explained by increasing lattice strain due to their ternary compositions.[19] The exact origin of the red shift is still unknown, and further investigations are needed.

To show their biological utility, core/shell CdHgTe/ZnS were coated with phospholipid micelles using a protocol developed previously.[2] This coating is known to suppress the toxicity of the NCs, render them water-soluble, allow bioactivity, and keep the quantum yields high. Live P815 mast cells were incubated with near-IR NCs (emission 728 nm) overnight and washed. Confocal laser microscopy images taken within a spectral range between 650 and 750 nm clearly show that the cells have been stained with NCs (Figure 3). Control experiments show no autofluorescence within the detection range. After 3 days of incubation the cells were still healthy and the IR fluorescence was still detectable. However, the NCs photobleached after repetitive laser scans. Other bioconjugation schemes that were developed for CdSe/ZnS NCs could also be used because of identical shell composition and environment.[20]

Nanocrystals synthesized using the hybrid approach are highly luminescent, stable for months in butanol, and have a higher resistance to photobleaching compared to cores (but they are not as photostable as CdSe/ZnS). The high quantum yield (over 50%) of these NCs is among the highest reported for the far-red region (670−700 nm). Quantum yields are also high (20−50%) in the near-IR region (>700 nm). This wavelength region is attractive for various biological applications because of reduced autofluorescence background, improved penetration into scattering tissue, and enhanced photostability.

Acknowledgment. This work was funded by the National Institute of Health, Grant No. R01 EB000312-04 and the Deutsche Forschungsgemeinschaft, PF 432/1-1. Confocal laser scanning microscopy was performed at the UCLA/CNSI Advanced Light Microscopy/Spectroscopy Shared Facility.

Supporting Information Available: Detailed nanocrystal synthesis procedures and X-ray diffraction data (PDF). This material is available free of charge via the Internet at http:/pubs.acs.org.

References

(1) Alivisatos, A. P. *Science* **1996**, *271*, 933.
(2) Dubertret, B.; Skourides, P.; Norris, D. J.; Noireaux, V.; Briovanlou, A. H.; Libchaber, A. *Science* **2002** *298*, 1759.
(3) Larson, D. R.; Zipfel, W. R. Williams, R. M.; Clark, S. W.; Bruchez, M. P.; Wise, F. W.; Webb, W. W. *Science* **2003**, *300*, 1434.
(4) Rogach, A. L.; Harrison, M. T.; Kershaw, S. V.; Kornowski, A.; Burt, M. G.; Eychmüller, A.; Weller, H. *Phys. Status Solidi B* **2001**, *224*, 1553.
(5) Kuno, Masaru; Higginson, K. A.; Qadri, S. B.; Yousuf, M.; Lee, S. H.; Davis, B. L.; Mattoussi, H. *J. Phys. Chem. B* **2003**, *107*, 5758.
(6) Hines, M. A.; Guoyot-Sionnest, P. *J. Phys. Chem.* **1996**, *100*, 468.
(7) Dabbousi, B. O.; Rodriguez Viejo, J.; Mikulec, F. V.; Heine, J. R.; Mattoussi, H.; Ober, R.; Jense, K. F.; Bawendi, M. G. *J. Phys. Chem. B* **1997**, *101*, 9463.
(8) Peng, X. G.; Schlamp, M. C.; Kadavanich, A. V.; Alivisatos, A. P. *J. Am. Chem. Soc.* **1997**, *119*, 7019.
(9) Pathak, S.; Choi, S.; Arnheim, N.; Thompson, M. *J. Am. Chem. Soc.* **2001**, *123*, 4103.
(10) Parak, W. J.; Gerion, D.; Zanchet, D.; Worez, A.; Pellgrino, T.; Micheel, C.; Williams, S. C.; Seitz, M.; Bruehl, R. E.; Bryant, Z.; Bustamante, C.; Bertozzi, C. R.; Alivisatos, A. P. *Chem. Mater*. **2002**, *14*, 2113.
(11) Akerman, M.; Chan, W. C. W.; Laakkonen, P.; Bhatia, S. N.; Ruoslahti, E. *Proc. Natl. Acad. Sci. U.S.A.* **2002**, Vol 99, *20*, 12617.
(12) Schroedter, A.; Weller, H.; Ertija, R.; Ford, W. E.; Wessels, J. M. *Nanoletters* **2002**, *2* (12), 1363.
(13) Goldman, E. R.; Balighian, E. D.; Mattoussi, H.; Kuno, M. K.; Mauro, J. M.; Tran, P. T.; Anderson, G. P. *J. Am. Chem. Soc*. **2002**, *124*, 6378.
(14) Harrison, M. T.; Kershaw, S. V.; Rogach, A. L.; Kornowski, A.; Eychmüller, A.; Weller, H. *Adv. Mater*. **2000**, *12*, 123.
(15) Kershaw, S. V.; Burt, M.; Harrison, M.; Rogach, A. L.; Eychmüller, A.; Weller, H. *Appl. Phys Lett.* **1999**, *75*, 1694−1696.
(16) Gaponik, N.; Talapin, D. V.; Rogach, A. L.; Eychmüller, A.; Weller, H. *Nanoletters* **2002**, *8*, 803.
(17) Rogach, A. L.; Katsikas, L.; Kornowski, A.; Su, D.; Eychmüller, A.; Weller, H. *Ber. Bunsen-Ges. Phys. Chem.* **1996**, *100* (11), 1772.
(18) Gaponik, N.; Talapin, D. V.; Rogach, A. L.; Hoppe, K.; Schevchenko, E. V.; Kornowski, A.; Eychmüller, A.; Weller, H. *J. Phys. Chem. B* **2002**, *106*, 7177.
(19) Bailey, R. E.; Nie, S. *J. Am. Chem. Soc.* **2003**, *125* (23), 7100.
(20) Pinaud, F.; King, D.; Moore, H.; Weiss, S. Manuscript in preparation.

JA039227V